

# A [<sup>1</sup>H, <sup>15</sup>N] Heteronuclear Single Quantum Coherence NMR Study of the Solution Reactivity of the Ruthenium-Based Mitochondrial Calcium Uniporter Inhibitor Ru265

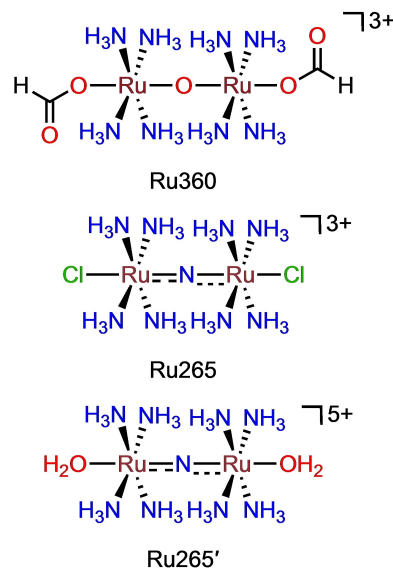
Joshua J. Woods,<sup>[a, b, c]</sup> Jesse A. Spivey,<sup>[a]</sup> and Justin J. Wilson<sup>\*[a]</sup>

The synthesis and characterization of the <sup>15</sup>N-labeled analogue of the mitochondrial calcium uptake inhibitor [Cl(NH<sub>3</sub>)<sub>4</sub>Ru(μ-N)Ru(NH<sub>3</sub>)<sub>4</sub>Cl]<sup>3+</sup> (Ru265) bearing [<sup>15</sup>N]NH<sub>3</sub> ligands is reported. Using [<sup>1</sup>H, <sup>15</sup>N] HSQC NMR spectroscopy, the rate constants for the axial chlorido ligand aquation of [<sup>15</sup>N]Ru265 in pH 7.4 buffer at 25 °C were found to be  $k_1 = (3.43 \pm 0.03) \times 10^{-4} \text{ s}^{-1}$  and  $k_2 = (4.03 \pm 0.09) \times 10^{-3} \text{ s}^{-1}$ . The reactivity of [<sup>15</sup>N]Ru265 towards biologically relevant small molecules was also assessed via this

method, revealing that this complex can form coordination bonds to anionic oxygen and sulfur donors. Time-based studies on these ligand-binding reactions reveal this process to be slow relative to the time required for the complex to inhibit mitochondrial calcium uptake, suggesting that hydrogen-bonding interactions, rather than the formation of coordination bonds, may play a more significant role in mediating the inhibitory properties of this complex.

## Introduction

Ruthenium 265 (Ru265), [Cl(NH<sub>3</sub>)<sub>4</sub>Ru(μ-N)Ru(NH<sub>3</sub>)<sub>4</sub>Cl]<sup>3+</sup>, is a potent and selective inhibitor of the mitochondrial calcium uniporter (MCU), the channel that mediates mitochondrial calcium uptake (Scheme 1).<sup>[1–3]</sup> This complex is an improved analogue of the widely-used MCU inhibitor Ru360, an oxo-bridged diruthenium complex of the formula [(HCCO<sub>2</sub>)(NH<sub>3</sub>)<sub>4</sub>Ru(μ-O)Ru(NH<sub>3</sub>)<sub>4</sub>(O<sub>2</sub>CCH)]<sup>3+</sup>.<sup>[4–7]</sup> Unlike Ru360, Ru265 can effectively inhibit the MCU in intact, non-permeabilized biological systems.<sup>[8–10]</sup> In contrast to the mixed-valent and paramagnetic Ru360, Ru265 contains two spin-coupled d<sup>4</sup> Ru<sup>4+</sup> centers, yielding a diamagnetic ground state<sup>[11,12]</sup> and making this complex amenable to characterization by NMR spectroscopy. Although the protons of the ammine ligands of Ru265 could be used to study the solution behavior of Ru265 by <sup>1</sup>H NMR spectroscopy, their signals are significantly broadened by the quadrupolar I = 1 <sup>14</sup>N nucleus. To overcome this limitation, we sought to prepare an isotopically labeled version of this complex, [<sup>15</sup>N]Ru265, in which the ammine ligands are enriched with the I = 1/2 <sup>15</sup>N isotope. This <sup>15</sup>N-labeled analogue allows for the investigation of the solution behavior of Ru265 by 2-



Scheme 1. Chemical Structures of Ru360, Ru265, and Ru265'.

dimensional [<sup>1</sup>H, <sup>15</sup>N] heteronuclear single quantum coherence nuclear magnetic resonance (HSQC NMR) spectroscopy, a technique that has been used extensively to study the solution reactivity of precious metal anticancer agents.<sup>[13–24]</sup> In this study, we report the synthesis and characterization of this isotopically labeled compound, and employ [<sup>1</sup>H, <sup>15</sup>N] HSQC NMR spectroscopy to study its axial chlorido ligand aquation kinetics, as well as its reactivity with several biologically relevant small molecules. Taken together, these results highlight the value of this spectroscopic technique for studying the solution reactivity of bioactive metal ammine complexes in biological environments.

[a] Dr. J. J. Woods, J. A. Spivey, Prof. J. J. Wilson  
Department of Chemistry and Chemical Biology,  
Cornell University,  
14853 Ithaca, NY, USA  
E-mail: jjw275@cornell.edu

[b] Dr. J. J. Woods  
Robert F. Smith School for Chemical and Biomolecular Engineering, Cornell  
University,  
14853 Ithaca, NY, USA

[c] Dr. J. J. Woods  
Present Address: Chemical Sciences Division,  
Lawrence Berkeley National Laboratory,  
94720 Berkeley, CA, USA

Supporting information for this article is available on the WWW under  
<https://doi.org/10.1002/ejic.202100995>

Part of the "YourJIC Talents" Special Collection.

## Results and Discussion

Although Ru265 is typically prepared via the action of concentrated aqueous  $\text{NH}_4\text{OH}$  on  $\text{K}_3[(\text{OH}_2)\text{Cl}_4\text{Ru}(\mu\text{-N})\text{RuCl}_4(\text{OH}_2)]$ , we sought alternative synthetic procedures that use the most readily available and affordable source of  $^{15}\text{N}$ , solid  $^{15}\text{N}[\text{NH}_4]\text{Cl}$ . Initial reactions involving this reagent were first optimized using unlabeled  $^{14}\text{NH}_4\text{Cl}$ . Notably, when  $\text{K}_3[(\text{H}_2\text{O})\text{Cl}_4\text{Ru}(\mu\text{-N})\text{RuCl}_4(\text{OH}_2)]$  was directly added to an aqueous solution containing a mixture of 7 M  $\text{NH}_4\text{Cl}$  and 7 M  $\text{NaOH}$ , a strategy that has been previously employed for the synthesis of  $^{15}\text{N}$ -labeled Pt complexes,<sup>[25,26]</sup> the reaction did not proceed. Similarly, the direct reaction between  $\text{NH}_4\text{Cl}$  and  $\text{K}_3[(\text{H}_2\text{O})\text{Cl}_4\text{Ru}(\mu\text{-N})\text{RuCl}_4(\text{OH}_2)]$  in water without added base did not yield the desired product. Thus, we rationalized that a concentrated aqueous solution of  $\text{NH}_4\text{OH}$  would be required to obtain the desired complex. Because concentrated solutions of  $^{15}\text{N}[\text{NH}_4]\text{OH}$  are prohibitively expensive, we generated gaseous  $^{15}\text{N}[\text{NH}_3]$  from  $^{15}\text{N}[\text{NH}_4]\text{Cl}$  by heating a solid mixture of this salt and excess  $\text{NaOH}$ .<sup>[27,28]</sup> The evolved gas was then bubbled through water to obtain a concentrated aqueous solution of  $^{15}\text{N}[\text{NH}_4]\text{OH}$  (Figure S1), which was applied for the successful synthesis of  $^{15}\text{N}[\text{Ru}265]$  from  $\text{K}_3[(\text{H}_2\text{O})\text{Cl}_4\text{Ru}(\mu\text{-N})\text{RuCl}_4(\text{OH}_2)]$  using  $^{15}\text{N}[\text{NH}_4]\text{Cl}$  as the source of  $^{15}\text{N}[\text{NH}_3]$ . The infrared spectrum of  $^{15}\text{N}[\text{Ru}265]$  is similar to that of Ru265, featuring a characteristic intense band near  $1050\text{ cm}^{-1}$  that corresponds to the asymmetric Ru–N–Ru stretching mode (Figure S2). Notably, a small red-shift in the N–H stretching modes is observed, consistent with the larger reduced mass afforded by the heavy  $^{15}\text{N}$  isotope. The  $^1\text{H}$  NMR spectrum of  $^{15}\text{N}[\text{Ru}265]$  in  $\text{DMSO-}d_6$  displays a relatively sharp doublet centered at 4.22 ppm with a coupling constant of 70 Hz. This resonance is assigned to the symmetry-equivalent protons of the  $^{15}\text{N}$ -labeled ammine ligands with the 70 Hz splitting arising from coupling of the  $^1\text{H}$  and  $^{15}\text{N}$  nuclei (Figure S3). The  $^{15}\text{N}\{^1\text{H}\}$  spectrum in  $\text{DMSO-}d_6$  displays a single resonance at  $-25.5$  ppm vs. liquid  $\text{NH}_3$  ( $\delta = 0$  ppm) (Figure S3). Similarly, the  $^{15}\text{N}$ -decoupled  $^1\text{H},^{15}\text{N}$  HSQC spectrum of  $^{15}\text{N}[\text{Ru}265]$  in 90:10  $\text{H}_2\text{O}/\text{D}_2\text{O}$  reveals a major  $^1\text{H}/^{15}\text{N}$  cross-peak at {4.10,  $-30.21$ } ppm, corresponding to the symmetry-equivalent ammine ligands of  $^{15}\text{N}[\text{Ru}265]$ , which is consistent with the X-ray crystal structure

of the complex (Scheme 1).<sup>[1]</sup> In addition to this major species, two minor peaks, assigned to the asymmetric ammine ligands of the partially aquated species  $[\text{ClRu}(\text{NH}_3)_4(\mu\text{-N})\text{Ru}(\text{NH}_3)_4(\text{OH}_2)]^{4+}$ , are observed at {4.18,  $-29.62$ } and {4.26,  $-29.97$ } ppm (Figure 1).

Although we have previously studied the aquation of Ru265 by UV-vis spectroscopy,<sup>[29]</sup> the direct observation of  $[\text{ClRu}(\text{NH}_3)_4(\mu\text{-N})\text{Ru}(\text{NH}_3)_4(\text{OH}_2)]^{4+}$  by  $^1\text{H},^{15}\text{N}$  HSQC NMR spectroscopy prompted us to reinvestigate this process. With our prior studies, only a single pseudo-first-order rate constant was determined even though the loss of the two chlorido ligands occurs through a step-wise process (Figure 2a). To gain insight on this stepwise process, we monitored the aquation reaction using  $^1\text{H},^{15}\text{N}$  HSQC NMR spectroscopy. The monosubstituted complex  $[\text{ClRu}(\text{NH}_3)_4(\mu\text{-N})\text{Ru}(\text{NH}_3)_4(\text{OH}_2)]^{4+}$  appears initially followed by the rapid formation of the diaquated product  $[(\text{H}_2\text{O})\text{Ru}(\text{NH}_3)_4(\mu\text{-N})\text{Ru}(\text{NH}_3)_4(\text{OH}_2)]^{5+}$  (Ru265', Scheme 1), which is characterized by a single crosspeak at {3.73,  $-29.56$ } ppm (Figure 2). The rate constants of the substitution reactions were determined by fitting these data to a series of first-order integrated rate laws for a sequential  $\text{A} \rightarrow \text{B} \rightarrow \text{C}$  reaction pathway (eqs 1–3).<sup>[30,31]</sup> The rate constants are  $k_1 = (3.43 \pm 0.03) \times 10^{-4} \text{ s}^{-1}$  and  $k_2 = (4.03 \pm 0.09) \times 10^{-3} \text{ s}^{-1}$ . Notably,  $k_1$  is almost an order of magnitude smaller than  $k_2$ , indicating that the first ligand substitution step is rate-determining. The value of  $k_1$  agrees well with the value of  $k_{\text{obs}}$  determined using UV-vis spectroscopy ( $2.59 \times 10^{-4} \text{ s}^{-1}$ ),<sup>[29]</sup> reflecting the fact that the latter measurements were unable to distinguish the mono- and diaquated species and could only resolve the first substitution reaction.

$$[\text{A}] = [\text{A}]_0 \exp(-k_1 t) \quad (1)$$

$$[\text{B}] = [\text{B}]_0 \exp(-k_2 t) + [\text{A}]_0 k_1 (k_2 - k_1)^{-1} \{ \exp(-k_1 t) - \exp(-k_2 t) \} \quad (2)$$

$$[\text{C}] = [\text{C}]_0 + [\text{B}]_0 \{ 1 - \exp(-k_2 t) \} + [\text{A}]_0 (1 + \{ k_1 \exp(-k_2 t) - k_2 \exp(-k_1 t) \} / (k_2 - k_1)) \quad (3)$$

We next sought to explore the utility of  $^1\text{H},^{15}\text{N}$  HSQC NMR spectroscopy to probe the solution speciation of  $^{15}\text{N}[\text{Ru}265]$ . These efforts were initiated by exploring the chemical shift changes of the ammine ligands of  $^{15}\text{N}[\text{Ru}265]$  as the axial ligands were varied. The acetate (OAc)-capped complex  $[(\text{AcO})(\text{NH}_3)_4\text{Ru}(\mu\text{-N})\text{Ru}(\text{NH}_3)_4(\text{OAc})]^{3+}$  ( $^{15}\text{N}[\text{RuOAc}]$ ) was synthesized as a model to probe the chemical shift changes of Ru265 in the presence of coordinating carboxylate donors. The  $^1\text{H},^{15}\text{N}$  HSQC NMR spectrum of  $^{15}\text{N}[\text{RuOAc}]$  features a single crosspeak at {4.06,  $-30.24$ } ppm, corresponding to the symmetry-equivalent ammine ligands of the disubstituted complex (Figure S4). Although this chemical shift is similar to that of the chlorido-capped  $^{15}\text{N}[\text{Ru}265]$ , it is appreciably different from its asymmetric monosubstituted analogues  $[\text{ClRu}(\text{NH}_3)_4(\mu\text{-N})\text{Ru}(\text{NH}_3)_4(\text{OH}_2)]^{4+}$  and  $[(\text{OAc})\text{Ru}(\text{NH}_3)_4(\mu\text{-N})\text{Ru}(\text{NH}_3)_4(\text{OH}_2)]^{4+}$ , and  $^{15}\text{N}[\text{Ru}265']$ , suggesting that  $^1\text{H},^{15}\text{N}$  HSQC NMR spectroscopy can be used to probe the axial ligand speciation of Ru265 in aqueous solution. We next explored the



Justin Wilson is an associate professor in the Department of Chemistry and Chemical Biology at Cornell University. His research program focuses broadly on the use of metals in medicine. Within this field, his research group is working in several areas, including the development of new metal-based anticancer agents, chelator design for radioactive metal ions, and ion channel inhibitors based on coordination complexes. The research of his group has been recognized by several awards, including the 2019 Cottrell Research Scholar Award, the 2019 Jonathan L. Sessler Award for Emerging Leaders in Bioinorganic and Medicinal Inorganic Chemistry, and the 2022 Harry Gray Award for Creative Work in Inorganic Chemistry by a Young Investigator.

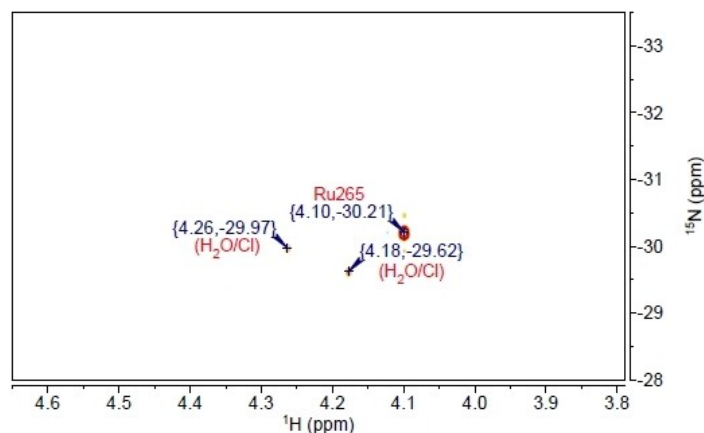


**Figure 1.** [ $^1\text{H},^{15}\text{N}$ ] HSQC NMR spectrum (600 MHz, 60.84 MHz, 25 °C) of [ $^{15}\text{N}$ ]Ru265 in 90:10  $\text{H}_2\text{O}/\text{D}_2\text{O}$ . The major crosspeak at {4.10, -30.21} ppm is assigned to [ $^{15}\text{N}$ ]Ru265, whereas the two minor crosspeaks at {4.18, -29.62} and {4.26, -29.97} ppm correspond to the mono-aquated species  $[\text{ClRu}(\text{NH}_3)_4(\mu\text{-N})\text{Ru}(\text{NH}_3)_4(\text{OH}_2)]^{4+}$ .

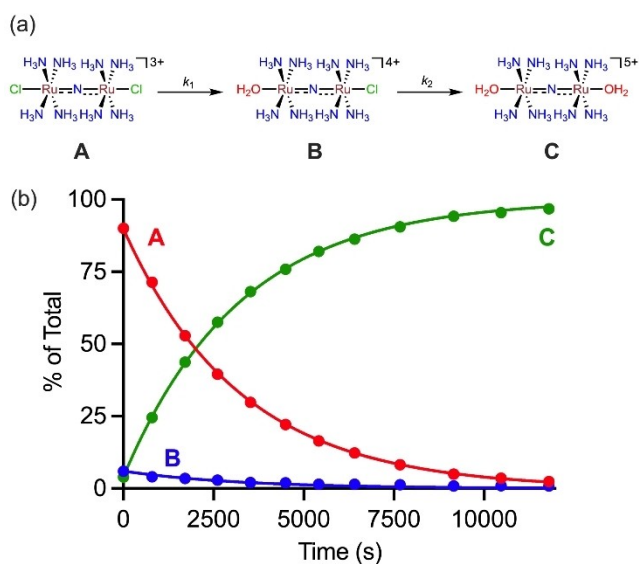


**Figure 2.** (a) Stepwise reaction and kinetic model used to fit concentration vs time data for the aquation of [ $^{15}\text{N}$ ]Ru265. (b) Representative concentration vs time data for the aquation of [ $^{15}\text{N}$ ]Ru265 at 25 °C ( $\text{p}(\text{H},\text{D}) = 7.4$ ) with the best fits to the integrated rate laws for a sequential  $\text{A} \rightarrow \text{B} \rightarrow \text{C}$  reaction (see equation 1, equation 2, and equation 3). Here  $\text{p}(\text{H},\text{D})$  is used to denote the pH of the 90:10  $\text{H}_2\text{O}/\text{D}_2\text{O}$  solution.<sup>[32]</sup>

[ $^1\text{H},^{15}\text{N}$ ] HSQC NMR chemical shift changes upon the treatment of [ $^{15}\text{N}$ ]Ru265 with several biologically relevant small molecules. This analysis was carried out by combining [ $^{15}\text{N}$ ]Ru265 with 10 equiv. of the desired ligand in 90:10  $\text{H}_2\text{O}/\text{D}_2\text{O}$  supplemented with 50 mM MOPS ( $\text{p}(\text{H},\text{D})$  7.4) and incubating the resulting solutions at 25 °C for 24 h prior to acquisition of the HSQC NMR spectra (Table 1 and Figures S5–S7). Although the use of 10 equiv. of the desired biomolecule is not biologically relevant, these conditions were chosen to identify ligands capable of coordinating to Ru265 through the axial positions.

For all ligands tested except *N*-methylimidazole, we observed the formation three additional crosspeaks in the [ $^1\text{H},^{15}\text{N}$ ]

HSQC NMR spectrum, which we assigned to the asymmetric mono- and symmetric disubstituted complexes. The lack of new crosspeaks in the spectrum of the *N*-methylimidazole reaction mixture suggests that this nitrogen donor is not an effective ligand for Ru265 and that nitrogen-donor amino acid residues, like histidine, are unlikely to coordinate this complex. In contrast, ligands containing oxygen and sulfur donors appear to bind to Ru265. A comparison of the relative ratios of [ $^{15}\text{N}$ ]Ru265', the monosubstituted, and disubstituted complexes provides a snapshot on the donor atom preferences of Ru265. In the presence of *N*-Boc-*L*-aspartic acid tert-butyl ester (NBocAspOtBu), the mono- and disubstituted complexes comprise 84% and 1.8% of the total Ru, respectively. In the case of *N*-acetyl-*L*-cysteine methyl ester, in which only the thiol donor is available for metal coordination, 87% of the total Ru remains as [ $^{15}\text{N}$ ]Ru265' with the mono- and disubstituted complexes making up the remaining 13%. When [ $^{15}\text{N}$ ]Ru265 was incubated with glutathione (GSH), a tripeptide with primary amine, carboxylate, and thiol donors, we observed multiple species in solution characterized by crosspeaks at {4.09, -29.62}, {4.06, -29.74}, {4.05, -29.74}, {4.05, -29.78}, {3.95, -30.60}, {3.82, -28.84}, {3.79, -28.88}, and {3.76, -29.58} ppm (Figure S7). The chemical shifts of these peaks are closer to those observed for carboxylate-capped species than those of the thiol-bound complex. Therefore, we hypothesize that Ru265 interacts with GSH through the terminal carboxylate groups rather than the thiol. These results demonstrate that chemical shifts of the equatorial ammine ligands of Ru265 are sensitive to the identity of the ligand in the axial positions and that Ru265 possesses a strong preference for ligands containing anionic oxygen donors over thiol- and nitrogen-based donors. Previously studied  $^{15}\text{N}$ -labeled Pt ammine complexes exhibit large changes in  $^{15}\text{N}$  chemical shifts ( $\geq 50$  ppm) as ligands *trans* to the ammine ligand are altered.<sup>[17]</sup> The  $^{15}\text{N}$  chemical shifts of the *cis* ammine ligands of Ru265 vary by less than 2 ppm in the presence of different axial ligands. These smaller chemical shift changes may limit the range of

**Table 1.** [<sup>1</sup>H,<sup>15</sup>N] HSQC NMR (600 MHz, 60.84 MHz, 90:10 H<sub>2</sub>O/D<sub>2</sub>O, p(H,D)=7.4, 50 mM MOPS, 25 °C) chemical shifts of [<sup>15</sup>N]Ru265 in the presence of biologically relevant ligands.

Axial Ligand	Monosubstituted (L/H <sub>2</sub> O)	Disubstituted (L/L)
H <sub>2</sub> O	–	{3.73, –29.56}
Cl	{3.86, –31.25}; {3.84, –28.36}	{4.03, –30.27}
CO <sub>3</sub> <sup>2–</sup>	{4.02, –29.21}; {3.79, –29.46}	{4.05, –29.09}
HPO <sub>4</sub> <sup>2–</sup>	– <sup>[a]</sup>	{4.00, –28.73}
NBocAspOtBu <sup>[b]</sup>	{3.92, –30.78}; {3.77, –28.94}	{4.03, –30.11}
GluOMe <sup>[c]</sup>	{3.95, –30.68}; {3.78, –29.07}	– <sup>[d]</sup>
NacCysOMe <sup>[e]</sup>	{3.96, –30.59}; {3.80, –28.82}	{3.96, –29.29}
N-Melm	NR <sup>[f]</sup>	NR

[a] Addition of Na<sub>2</sub>HPO<sub>4</sub> to the Ru265 solution led to precipitation with a small amount of complex remaining in solution. Peaks for the monosubstituted complex were not observed. <sup>31</sup>P NMR spectroscopy confirmed complexation (Figure S6). [b] *N*-Boc-*L*-aspartic acid *tert*-butyl ester. [c] *L*-glutamic acid methyl ester. [d] The resonance corresponding to the disubstituted complex could not be definitively assigned. [e] *N*-acetyl-*L*-cysteine methyl ester. [f] No reaction

experiments that can be used to determine the speciation of [<sup>15</sup>N]Ru265 in more complex biological solutions.

We have recently shown that the MCU-inhibitory activity of Ru265 is dependent on the aspartate residue D261 in human MCU; mutation of this residue significantly reduces the potency of the compound.<sup>[10]</sup> This aspartate residue resides on an exposed surface of the MCU within an amino acid sequence that is known as the DIME region. The exact role of D261 on the mechanism of action of Ru265 remains unclear, and we sought to explore the possibility that Ru265 could form a coordination bond with D261. To this end, a solution of [<sup>15</sup>N]Ru265 was treated with a peptide model of the solvent-exposed region of the MCU (MCU-DIME; Figure 3). After 24 h, the [<sup>1</sup>H,<sup>15</sup>N] HSQC spectrum of [<sup>15</sup>N]Ru265 and MCU-DIME showed that Ru265' comprised the majority (86%) of the total Ru in solution. We also observed two smaller crosspeaks at {4.02, –29.87} and {3.99, –29.91}, which totaled to 8% and 6% of the overall

integrated peak intensity, respectively (Figure 3). Because these chemical shifts closely match those of the reaction products of [<sup>15</sup>N]Ru265 with anionic oxygen donor ligands (Table 1), these peaks most likely correspond to carboxylate-capped derivatives of Ru265, suggesting the potential for binding of this complex to the peptide.

To further investigate the role of coordination bonding in the MCU-inhibitory properties of Ru265, we monitored the rate at which this compound binds to NBocAspOtBu. The HSQC NMR spectra of [<sup>15</sup>N]Ru265 in the presence of 10 equiv. of NBocAspOtBu at 25 °C were acquired at 1, 5, and 24 h. After 1 h, only crosspeaks corresponding to [<sup>15</sup>N]Ru265 and [<sup>15</sup>N]Ru265' were observed. After incubating for 5 h, peaks corresponding to the asymmetric [(NBocAspOtBu)(NH<sub>3</sub>)<sub>4</sub>Ru(μ-N)Ru(NH<sub>3</sub>)<sub>4</sub>(OH<sub>2</sub>)<sup>4+</sup> complex, which comprised approximately 60% of the total Ru in solution, were observed with the remaining 40% existing as [<sup>15</sup>N]Ru265' (Figure S8). Thus, the formation of coordination

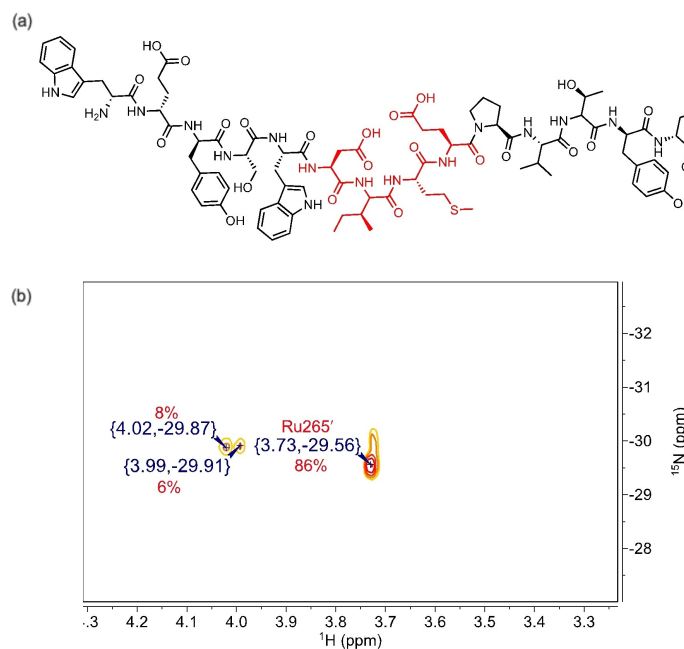


**Figure 3.** (a) Chemical structure of MCU-DIME (WEYSWDIMEPVTYF). The DIME motif is highlighted in red. (b) [<sup>1</sup>H,<sup>15</sup>N] HSQC NMR spectrum (600 MHz, 60.84 MHz, 25 °C, 90:10 H<sub>2</sub>O/D<sub>2</sub>O + 50 mM MOPS, p(H,D) = 7.4) of [<sup>15</sup>N]Ru265 incubated for 24 h at 25 °C in the presence of 2 equiv. of MCU-DIME.

bonds with carboxylate-containing amino acid residues occurs on a relatively slow timescale. In this context, we have previously shown that the addition of Ru265 to permeabilized cells at 25 °C results in an immediate cessation of mitochondrial  $\text{Ca}^{2+}$  uptake and that inhibition of the MCU by Ru265 is fully reversible.<sup>[10]</sup> Given that no appreciable complexation was observed within 1 h, it appears unlikely that coordination of Ru265 to this residue mediates the MCU-inhibitory activity of this complex. Outer-sphere hydrogen-bonding interactions, as suggested by our recent molecular docking studies,<sup>[10]</sup> seem more likely to play an operative role in the MCU-inhibitory activity of this complex. Further investigation of the interactions between Ru265 and the isolated MCU protein will be required to verify this hypothesis given that the complex may react differently in the protein environment of the intact MCU pore and is currently underway in our lab.

## Conclusion

In summary, we have prepared an  $^{15}\text{N}$ -labeled analogue of the Ru-based MCU inhibitor Ru265. This complex was used to study the solution reactivity of Ru265 with biologically relevant small molecules via [ $^1\text{H}$ , $^{15}\text{N}$ ] HSQC NMR spectroscopy. These studies revealed that Ru265 can form coordination bonds with anionic oxygen donors preferably over softer sulfur and nitrogen-based donors. In addition, we studied the interaction of [ $^{15}\text{N}$ ]Ru265 with a peptide model of the DIME region of the MCU. Although these experiments showed that Ru265 can form coordination bonds with this peptide, the timescale of this process was significantly longer than that required for its mitochondrial  $\text{Ca}^{2+}$  uptake inhibitory activity, suggesting that these types of interactions are not critical for its function. Future work will focus on using [ $^1\text{H}$ , $^{15}\text{N}$ ] HSQC NMR spectroscopy to study the biological speciation of Ru265 in more complex solutions and on leveraging knowledge obtained from these studies for the design of improved MCU inhibitors.

## Experimental Section

All reagents and solvents were obtained commercially and used without further purification unless otherwise noted. The MCU-DIME peptide (WEYSWDIMEPVYF) was custom synthesized by BioMatik (Wilmington, DE). Deionized water ( $\geq 18 \text{ M}\Omega\cdot\text{cm}$ ) was obtained from an Elga Purelab Flex 2 water purification system. The complex  $\text{K}_3[(\text{H}_2\text{O})\text{Cl}_4\text{Ru}(\mu\text{-N})\text{RuCl}_4(\text{OH}_2)]$  was synthesized by literature procedures.<sup>[11]</sup>

All 1D NMR spectra were obtained at 25 °C using a Bruker AV III HD 500 MHz spectrometer equipped with a broadband Prodigy cryoprobe. Chemical shifts are reported in ppm and were referenced to the residual solvent signal vs tetramethylsilane (TMS) at 0 ppm. Samples in  $\text{D}_2\text{O}$  were spiked with 0.1% 1,4-dioxane as an internal chemical shift reference ( $\delta = 3.75 \text{ ppm}$ ). Heteronuclear spectra were referenced indirectly to the corresponding  $^1\text{H}$  spectrum using the absolute reference function as implemented in MestReNova (Mestrelab Research, S.L). The 2D NMR spectra of [ $^{15}\text{N}$ ]Ru265 were acquired on a 600 MHz Varian INOVA spectrometer equipped with a 5 mm HCN inverse probehead operating at 599.50 MHz for  $^1\text{H}$  and

60.74 MHz for  $^{15}\text{N}$ . All samples were prepared so that the final solvent composition was 90:10  $\text{H}_2\text{O}/\text{D}_2\text{O}$  and were buffered to a final p(H,D) of 7.4 with 50 mM MOPS. Chemical shifts in the  $^1\text{H}$  dimension were referenced to 0.1% dioxane as an internal standard and are reported relative to  $\text{Me}_4\text{Si}$ . Shifts in the  $^{15}\text{N}$  dimension were referenced indirectly to the corresponding  $^1\text{H}$  spectrum using the absolute reference function as implemented in MestReNova and are reported relative to liquid  $\text{NH}_3$  set at  $\delta = 0 \text{ ppm}$ .<sup>[33]</sup>  $^1\text{H}$  NMR spectra were acquired with water suppression using the WET pulse sequence as provided in *VnmrJ*. All 2D spectra (optimized for  $J(^{15}\text{N},^1\text{H}) = 70 \text{ Hz}$ ) were recorded at 298 K using the standard Varian pulse sequence HSQCAD as provided in *VnmrJ* (ver. 3.2) with a spectral width of 2397.9 Hz in the  $^1\text{H}$  direction and 1214.9 Hz in the  $^{15}\text{N}$  direction using an acquisition time of 0.150 s, a relaxation delay of 1 s, and a pulse width of 7.5 kHz. The [ $^1\text{H}$ , $^{15}\text{N}$ ] HSQC NMR spectra were decoupled by irradiating with the GARP-1 sequence during the acquisition time. The 2D spectra were processed using Gaussian weighting functions in both dimensions and zero-filling by  $\times 2$  in both dimensions as implemented in MestReNova. Infrared spectra were recorded using a Bruker Tensor II Infrared Spectrometer equipped with a diamond ATR crystal (Bruker, Billerica, MA). Elemental analyses (C, H, N) were carried out by Atlantic Microlab Inc. (Norcross, GA).

**Synthesis of [ $^{15}\text{N}$ ]Ru265.** Solid [ $^{15}\text{N}$ ]NH $_4$ Cl (3.044 g, 55.8 mmol) and NaOH (6.46 g, 161.5 mmol) were placed into a two-necked flask that was connected to a bubbler containing 10 mL  $\text{H}_2\text{O}$ . These solids were continuously heated with a heat gun to generate gaseous [ $^{15}\text{N}$ ]NH $_3$ , which was collected in the bubbler as a concentrated aqueous solution of [ $^{15}\text{N}$ ]NH $_4$ OH. The resulting aqueous solution of [ $^{15}\text{N}$ ]NH $_4$ OH was transferred to a thick-walled pressure vessel containing  $\text{K}_3[(\text{H}_2\text{O})\text{Cl}_4\text{Ru}(\mu\text{-N})\text{RuCl}_4(\text{OH}_2)]$  (87.3 mg, 0.133 mmol). The reaction was sealed and heated at 75 °C behind a blast shield for 48 h to give a bright orange solution with a small amount of tan precipitate. Upon cooling, the solids were removed by filtration, and the filtrate was evaporated under reduced pressure. The resulting solid was redissolved in minimal boiling water, and then precipitated with an equivalent volume of concentrated HCl. The solid was collected by centrifugation, suspended in 6 M HCl (6 mL), and reisolated by centrifugation twice. This centrifugation process was repeated with  $2 \times 6 \text{ mL}$  cold water, followed by  $2 \times 6 \text{ mL}$  acetone. The resulting orange solid was dried under vacuum. Yield: 49.1 mg (0.086 mmol, 64.6%).  $^1\text{H}$  NMR (500 MHz, DMSO- $d_6$ , 25 °C)  $\delta = 4.22$  (d,  $^1J_{\text{NH}} = 71 \text{ Hz}$ ,  $\text{NH}_3$ ) ppm.  $^{15}\text{N}$  [ $^1\text{H}$ ] NMR (50.6 MHz, DMSO- $d_6$ , 25 °C)  $\delta = -25.52$  ppm. IR (ATR)  $\nu = 3240$  (m), 3130 (m), 1600 (m), 1276 (s), 1050 (s), 824 (s), 794 (m), 736 (w)  $\text{cm}^{-1}$ . Elemental Analysis Calcd for  $\text{H}_{24}\text{Cl}_5\text{N}_9\text{Ru}_2 \cdot 3\text{H}_2\text{O}$ : C 0; H 5.18; N 21.60, found C 0.14; H 4.62; N 21.29.

**Reaction between [ $^{15}\text{N}$ ]Ru265 and NaOAc.** A solution of AgOTf (0.0236 g, 0.092 mmol) in water (2 mL) was added to a suspension of [ $^{15}\text{N}$ ]Ru265 (0.0105 g, 0.018 mmol) in water (4 mL), and the resulting mixture was stirred at 50 °C in the dark for 2 h. The precipitated AgCl was removed by filtration through a 0.2  $\mu\text{m}$  syringe filter, and sodium acetate (0.0032 g, 0.039 mmol) was added to the filtrate. The resulting solution was stirred at 50 °C for 18 h, yielding a yellow-orange solution. This solution was centrifuged, and the supernatant was lyophilized to give a yellow powder, which was analyzed by [ $^1\text{H}$ , $^{15}\text{N}$ ] HSQC NMR spectroscopy without further purification. [ $^1\text{H}$ , $^{15}\text{N}$ ] HSQC NMR (600 MHz, 60.8 MHz, 25 °C, 90:10  $\text{H}_2\text{O}/\text{D}_2\text{O}$  + 50 mM MOPS):  $\delta = \{4.06, -30.24\} \text{ ppm}$ .

**Aquation of [ $^{15}\text{N}$ ]Ru265.** A fresh solution of [ $^{15}\text{N}$ ]Ru265 was prepared at a typical concentration of 1 mM in 90:10  $\text{H}_2\text{O}/\text{D}_2\text{O}$ . buffered to a final p(H,D) of 7.4 with 50 mM MOPS containing 0.1% 1,4-dioxane in a total volume of 600  $\mu\text{L}$ . The p(H,D) of the sample was checked by pH paper to ensure that the solution remained buffered at the desired p(H,D).  $^1\text{H}$  and [ $^1\text{H}$ , $^{15}\text{N}$ ] HSQC NMR spectra



were recorded at 25 °C over a period of 4–5 h. The kinetic analysis of the aquation reaction was performed by fitting the peak volumes in the 2D spectra and calculating the relative concentrations of the <sup>15</sup>N-species at each time point. The aquation data were simultaneously fit with equations 1–3 using the nonlinear curve fitting procedure of GraphPad Prism 9 (GraphPad Software, LLC) to determine the values of  $k_1$  and  $k_2$ . Data are represented as the mean  $\pm$  SD ( $n=3$ ).

**Interaction with Biologically Relevant Ligands.** A fresh solution of [<sup>15</sup>N]Ru265 was prepared at a typical concentration of 1 mM in in 90:10 H<sub>2</sub>O/D<sub>2</sub>O buffered to a final p(H,D) of 7.4 with 50 mM MOPS containing 0.1% 1,4-dioxane in the presence of 10 equiv. of the desired biologically relevant species (2 equiv. for MCU-DIME) in a total volume of 600  $\mu$ L. The p(H,D) of the sample was checked by pH paper to ensure that the solution remained buffered at the desired p(H,D). The solution was then incubated for the desired time before the <sup>1</sup>H and [<sup>1</sup>H-<sup>15</sup>N] HSQC NMR spectra were recorded as described above.

## Acknowledgements

The work was supported by the American Heart Association (AHA Predoctoral Fellowship to J. J. Woods, Award No. 20PRE35120390) and the National Science Foundation (NSF CAREER Award for J. J. Wilson, Award No. CHE-1750295). Dr. Ivan Keresztes is thanked for his assistance in setting up the [<sup>1</sup>H, <sup>15</sup>N] HSQC NMR experiments and for helpful discussions of the project. This work made use of the Cornell NMR facility, which is supported in part by the National Science Foundation (Award No. CHE-1531632).

## Conflict of Interest

The authors declare no conflict of interest.

## Data Availability Statement

The data that support the findings of this study are available in the supplementary material of this article.

**Keywords:** Bioinorganic chemistry · Heteronuclear single quantum coherence · NMR spectroscopy · Peptides · Ruthenium

- [2] J. M. Baughman, F. Perocchi, H. S. Girgis, M. Plovanich, C. A. Belcher-Timme, Y. Sancak, X. R. Bao, L. Strittmatter, O. Goldberger, R. L. Bogorad, V. Koteliansky, V. K. Mootha, *Nature* **2011**, *476*, 341–345.
- [3] K. J. Kamer, V. K. Mootha, *Nat. Rev. Mol. Cell Biol.* **2015**, *16*, 545–553.
- [4] M. A. Matlib, Z. Zhou, S. Knight, S. Ahmed, K. M. Choi, J. Krause-Bauer, R. Phillips, R. Altschuld, Y. Katsube, N. Sperelakis, D. M. Bers, *J. Biol. Chem.* **1998**, *273*, 10223–10231.
- [5] J. Emerson, M. J. Clarke, W. L. Ying, D. R. Sanadi, *J. Am. Chem. Soc.* **1993**, *115*, 11799–11805.
- [6] W.-L. Ying, J. Emerson, M. J. Clarke, D. Rao Sanadi, *Biochemistry* **1991**, *30*, 4949–4952.
- [7] S. R. Nathan, N. W. Pino, D. M. Arduino, F. Perocchi, S. N. MacMillan, J. J. Wilson, *Inorg. Chem.* **2017**, *56*, 3123–3126.
- [8] M. Kerkhofs, R. La Rovere, K. Welkenhuysen, A. Janssens, P. Vandenberghe, M. Madesh, J. B. Parys, G. Bultynck, *Cell Calcium* **2021**, *94*, 102333.
- [9] R. J. Novorolsky, M. Nichols, J. S. Kim, E. V. Pavlov, J. J. Woods, J. J. Wilson, G. S. Robertson, *J. Cereb. Blood Flow Metab.* **2020**, *40*, 1172–1181.
- [10] J. J. Woods, M. X. Rodriguez, C.-W. Tsai, M.-F. Tsai, J. J. Wilson, *Chem. Commun.* **2021**, *57*, 6161–6164.
- [11] M. J. Cleare, W. P. Griffith, *J. Chem. Soc. A* **1970**, 1117–1125.
- [12] J. D. Dunitz, L. E. Orgel, *J. Chem. Soc.* **1953**, 2594–2596.
- [13] R. A. Ruhayel, S. J. Berners-Price, N. P. Farrell, *Dalton Trans.* **2013**, *42*, 3181–3187.
- [14] Y. Qu, R. G. Kipping, N. P. Farrell, *Dalton Trans.* **2015**, *44*, 3563–3572.
- [15] S. J. Berners-Price, L. Ronconi, P. J. Sadler, *Prog. Nucl. Magn. Reson. Spectrosc.* **2006**, *49*, 65–98.
- [16] T. Zou, P. J. Sadler, *Drug Discovery Today Technol.* **2015**, *16*, 7–15.
- [17] Y. Kasherman, S. Sturup, D. Gibson, *J. Med. Chem.* **2009**, *52*, 4319–4328.
- [18] M. S. Davies, S. J. Berners-Price, T. W. Hambley, *J. Am. Chem. Soc.* **1998**, *120*, 11380–11390.
- [19] L. Cubo, D. S. Thomas, J. Zhang, A. G. Quiroga, C. Navarro-Ranninger, S. J. Berners-Price, *Inorg. Chim. Acta.* **2009**, *362*, 1022–1026.
- [20] A. I. Ivanov, J. Christodoulou, J. A. Parkinson, K. J. Barnham, A. Tucker, J. Woodrow, P. J. Sadler, *J. Biol. Chem.* **1998**, *273*, 14721–14730.
- [21] R. A. Ruhayel, B. Corry, C. Braun, D. S. Thomas, S. J. Berners-Price, N. P. Farrell, *Inorg. Chem.* **2010**, *49*, 10815–10819.
- [22] A. J. Di Pasqua, C. R. Centerwall, D. J. Kerwood, J. C. Dabrowiak, *Inorg. Chem.* **2009**, *48*, 1192–1197.
- [23] S. J. Berners-Price, T. A. Frenkiel, U. Frey, J. D. Ranford, P. J. Sadler, *J. Chem. Soc. Chem. Commun.* **1992**, *8*, 789–791.
- [24] H. K. Liu, J. A. Parkinson, J. Bella, F. Wang, P. J. Sadler, *Chem. Sci.* **2010**, *1*, 258–270.
- [25] M. Alei, P. J. Vergamini, W. E. Wageman, *J. Am. Chem. Soc.* **1979**, *101*, 5415–5417.
- [26] C. Boreham, J. Broomhead, D. Fairlie, *Aust. J. Chem.* **1981**, *34*, 659.
- [27] R. A. Woltonist, D. B. Collum, *J. Am. Chem. Soc.* **2020**, *142*, 6852–6855.
- [28] N. C. Thomas, *J. Chem. Educ.* **1990**, *67*, 431.
- [29] J. J. Woods, J. Lovett, B. Lai, H. H. Harris, J. J. Wilson, *Angew. Chem. Int. Ed.* **2020**, *59*, 6482–6491; *Angew. Chem.* **2020**, *132*, 6544–6553.
- [30] A. P. King, H. A. Gellineau, S. N. Macmillan, J. J. Wilson, *Dalton Trans.* **2019**, *48*, 5987–6002.
- [31] G. I. Gellene, *J. Chem. Educ.* **1995**, *72*, 196–199.
- [32] K. A. Rubinson, *Anal. Methods* **2017**, *9*, 2744–2750.
- [33] J. L. Markley, A. Bax, Y. Arata, C. W. Hilbers, R. Kaptein, B. D. Sykes, P. E. Wright, K. Wüthrich, *Eur. J. Biochem.* **1998**, *256*, 1–15.

[1] J. J. Woods, N. Nemani, S. Shanmughapriya, A. Kumar, M. Zhang, S. R. Nathan, M. Thomas, E. Carvalho, K. Ramachandran, S. Srikantan, P. B. Stathopoulos, J. J. Wilson, M. Madesh, *ACS Cent. Sci.* **2019**, *5*, 153–166.

Manuscript received: November 21, 2021  
Revised manuscript received: December 23, 2021  
Accepted manuscript online: December 30, 2021

